Dynamics of Spermatogenesis and Change in Testicular Morphology under 'Mating' and 'Non-Mating' Conditions in Medaka (Oryzias latipes)

Authors: Sumita, Ruka, Nishimura, Toshiya, and Tanaka, Minoru

Source: Zoological Science, 38(5) : 436-443

Published By: Zoological Society of Japan

URL: https://doi.org/10.2108/zs210025

ZOOLOGICAL SCIENCE **38**: 436–443 (2021)

Dynamics of Spermatogenesis and Change in Testicular Morphology Under 'Mating' and 'Non-mating' Conditions in Medaka (*Oryzias latipes*)

Ruka Sumita†, Toshiya Nishimura‡, and Minoru Tanaka*

Division of Biological Sciences, Graduate School of Science, Nagoya University, Nagoya 464-8602, Japan

Here, we report that the gross morphology of the testes changes under 'non-mating' or 'mating' conditions in medaka (*Oryzias latipes*). During these conditions, an efferent duct expands and a histological unit of spermatogenesis, the lobule, increases its number under 'non-mating' conditions. Based on BrdU labeling experiments, lower mitotic activity occurs in gonial cells under 'non-mating' conditions, which is consistent with the reduced number of germ cell cysts. Interestingly, the total number of type A spermatogonia was maintained, regardless of the mating conditions. In addition, the transition from mitosis to meiosis may have been retarded under the 'non-mating' conditions. The minimum time required for germ cells to become sperm, from the onset of commitment to spermatogenesis, was approximately 14 days in vivo. The time was not found to significantly differ between 'non-mating' and 'mating' conditions. The collective data suggest the presence of a mechanism wherein the homeostasis of spermatogenesis is altered in response to the mating conditions.

Key words: gametogenesis, mating conditions, spermatogonia, mitotic activity, efferent duct, environment

INTRODUCTION

Many environmental factors affect reproduction, including behavior, sexual maturity, and gametogenesis, at various levels. Further, temperature, photoperiod, and nutrition are well-known factors that affect reproduction (Shimizu et al., 2000; Sakae et al., 2020; Sakae and Tanaka, 2021). In fish and birds, the presence or absence of a mating partner can also be a factor (Munakata and Kobayashi, 2010; Tobari and Tsutsui, 2019). However, most of the mechanisms controlling reproduction in response to these factors remain unclear.

Medaka (*Oryzias latipes*) is a small fish used to study reproduction (Kinoshita et al., 2009). The sex is determined genetically, and once maturated under long photoperiod conditions, female medaka spawn eggs every day for several months (Kinoshita et al., 2009). Notably, the histological structure (germinal cradle) underlying the dynamics of oogenesis among vertebrates was first discovered in medaka (Nakamura et al., 2010; Nishimura et al., 2016). The cellular and molecular mechanisms regulating germline stem cells have been assessed (Nakamura et al., 2010, 2012).

* Corresponding author. E-mail: mtanaka@bio.nagoya-u.ac.jp
† Present address: SUN MEDICAL CO., LTD., Shiga 524-0044, Japan
‡ Present address: Faculty of Fisheries Sciences, Hokkaido University, Hakodate 041-8611, Japan
doi:10.2108/zs210025

The histological units of spermatogenesis in medaka testes are called lobules and they have been well documented (Onitake et al., 1972; Satoh, 1974; Grier, 1975; Kanamori et al., 1985). Lobules radiate from an efferent duct located in the middle of the testis (Kinoshita et al., 2009; Nishimura et al., 2016) (Fig. 1A). Type A spermatogonia containing germline stem cells are located in the most distal part of the lobule (Fig. 1B). Once spermatogonia are committed to spermatogenesis, they mitotically divide several times to increase their number. Thereafter, they undergo meiosis, producing primary and secondary spermatocytes. After the meiotic process, germ cells reach a stage of round spermatids, followed by the development of sperm through a metamorphic process of spermiogenesis. Spermatogonia with a population of germline stem cells continuously provide sperm. Thus, male medaka retain fertility during the reproductive period.

The dynamics of medaka spermatogenesis were analyzed in culture systems using isolated germ cells (Iwasaki et al., 2009). Several gene products affect the course of spermatogenesis (Watanabe et al., 1998; Schulz et al., 2010). However, the dynamics of spermatogenesis in vivo are unclear. We happened to find a change in testis structure in the presence or absence of a female partner. Owing to such observation, the present study was carried out to analyze the histological difference between the two mating conditions ('mating' and 'non-mating'). Here we define the term, 'mating', as the conditions in which a male is maintained in a tank with a female and successfully has the female spawn fertilized eggs every day, and the term, 'non-mating', as the

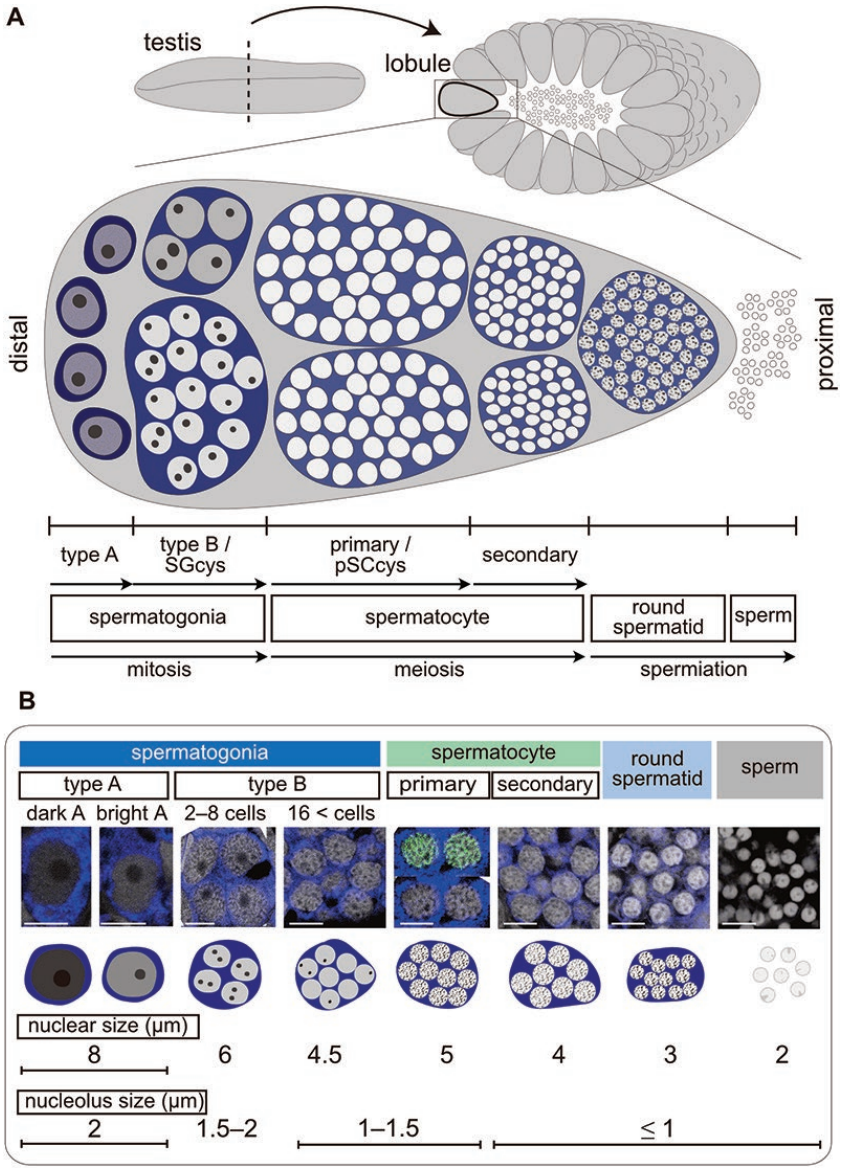

Fig. 1. The structure of the testis and lobule. **(A)** The testes are comprised of units called lobules. Spermatogenesis proceeds from the distal to the proximal side. **(B)** Characteristics of germ cells in each differentiation stage (bar, 5 μm; white, DAPI; blue, OLVAS; green, SYCP1; SGcys, cyst of type B spermatogonia; pSCcys, cyst of primary spermatocyte).

conditions in which a male is kept separated from females during a period of experiments (for the details, see Supplementary Figure S1A).

MATERIALS AND METHODS

Medaka strain and maintenance

The OK-Cab strain was maintained at 25°C under a 14 h light and 10 h dark photoperiod schedule. For males designated as 'mating male', the ability to fertilize eggs was confirmed every day by pair-mating with a female for 2 weeks before the onset of the experiments. For a 'non-mating male', sperm fertility was confirmed by pair-mating with a female for 2 weeks. Thereafter, the males were isolated individually in tanks for another 2 weeks until the experiments began (see Supplementary Figure S1A). The age of the male medaka used herein was 5 to 7 months post-hatching, with an average body length of 23.7 ± 0.8 mm (n = 18, the length was measured when they were dissected). All the medaka in this study were treated following the guidelines of the Animal Care and Use Committee in Nagoya University (approval number Sci 8).

Sex-genotyping

The genetic sex of all the medaka employed in our experiments was genotyped using *Dmy* Taqman primers, according to a previous study (Kikuchi et al., 2020).

Histology of testis

Whole testes were fixed in 4% paraformaldehyde (PFA, Wako, Osaka, Japan) at 4°C overnight and dehydrated in 100% methanol (Kanto Kagaku, Tokyo, Japan) at −30°C until use. The 4 μm sections were prepared as previously described using Technovit 8100 (KULZER, Hanau, Germany) plastic resin (Nishimura et al., 2018) and were stained with 1% neutral red (Wako).

Immunohistochemistry

Medaka testes were cut perpendicularly to the anterior-posterior axis into several pieces and fixed with 4% PFA overnight at 4°C. The fragments were dehydrated in 100% methanol (Kanto Kagaku) at −30°C until the performance of immunohistochemistry. Immunostaining was performed as previously described (Nakamura et al., 2006).

The following antibodies (all diluted 1/200) were used: rat anti-OLVAS serum without purification (Aoki et al., 2008); rabbit anti-SYCP1 serum without purification (Iwai et al., 2006); rabbit anti-Laminin polyclonal antibody (Sigma-Aldrich, St. Louis, USA, cat. # L9393); rabbit anti-bromodeoxyuridine (BrdU) mouse polyclonal antibody (SCB, Dallas, USA, cat. # sc-32323); anti-rat Alexa 488 conjugate (Thermo Fischer Scientific, Waltham, USA, cat. # A-11029); anti-mouse Alexa 488 conjugate (Thermo Fischer Scientific, cat. # A-11029); anti-rat Alexa 647 conjugate (Thermo Fischer Scientific, cat. # A-21247); and anti-rabbit Alexa 568 conjugate (Thermo Fischer Scientific, cat. # A-11036).

Before observation, the samples were stained with a 1/200 dilution of 4′,6-diamidino-2-phenylindole (DAPI, Thermo Fischer Scientific). The samples were further sliced into 0.2 to 0.4 mm thick sections. The sections were placed between two rows of dikes made with vinyl tape on a glass slide, with the cut surface of each section facing upward toward the objective lens of the microscope (see Supplementary Figure S1B). The area demarcated by dikes was embedded with Vectashield (Vector Labs, California, US) and covered with a coverslip. Observations were performed via confocal microscopy using a model FV1000 microscope (Olympus, Tokyo, Japan) equipped with a 60× objective lens (UPlanSApo, NA: 1.35, Olympus) and 100× objective lens (UPlanSApo, NA: 1.4, Olympus).

Pulse chase experiment

'Mating' and 'non-mating' males were maintained for 30 h (the time required for all mitotic germ cells to divide) in water containing 80 μM BrdU (SCB, see Supplementary Figure S1C). The treated

males were transferred to freshwater tanks and maintained until they were sacrificed.

Long term labeling experiment

'Mating' and 'non-mating' male medaka were maintained for 1 hour post BrdU treatment (hpB), 3 hpB, 1 day post BrdU treatment (dpB), 3 dpB, and 8 dpB in water containing 80 μM BrdU before sacrificing for gonad histology analysis (see Supplementary Figure S1A). During treatment, 'mating' males were paired with females and fertilized eggs were confirmed every day. 'Non-mating' males were kept alone in the tanks.

Enumeration of germ cells

A model FV-ASW microscope (Olympus) was used to count the number of germ cells. The given area was calculated using ImageJ software (NIH, Bethesda, US). Based on the raw data, graphs were plotted using OriginPro software (OriginLab, Northampton, US). Cysts were enumerated as a unit of germ cells connected by cytoplasm, which were further demarcated by Sertoli cells, regardless of the number of germ cells inside.

RESULTS

Identification of the spermatogenic stages of germ cells and definition of terms

The germ cells located in the most distal area of the lobules were identified as type A spermatogonia (Fig. 1A, B). These cells are characterized by their presence in isolation, with large cell volume and large nucleus (8 μm in diameter). Further, these cells should include a population of germline stem cells. The nucleus of type A spermatogonia has a single nucleolus with a size of 2 μm. Type A spermatogonia could be divided into two types (dark A and bright A) based on the intensity of DAPI staining (Fig. 1B). These two types have been observed in mammals (Fayomi and Orwig, 2018). In this study, the two types are collectively referred to as type A spermatogonia.

Interestingly, the average number of bright A spermatogonia in a single lobule was approximately seven-fold higher than that of dark A spermatogonia (see Supplementary Figure S2A). The ratio of dark A spermatogonia in the total number of type A spermatogonia in a single lobule was 15% (see Supplementary Figure S2B). No correlation was evident between the number of dark A and bright A spermatogonia in each lobule (see Supplementary Figure S2C).

Mitotically dividing germ cells, generally called type B spermatogonia, are present in groups (cysts) in which type B spermatogonia are surrounded by Sertoli cells and are connected to each other with an intercellular bridge (Saito et al., 2007; Nishimura et al., 2016) (Fig. 1A, B). A group of packed type B spermatogonia is collectively referred to as a cyst of type B spermatogonia (SGcys) in this study. Type B spermatogonia in SGcys displayed a smaller volume than type A spermatogonia with a smaller nucleus (5–6 μm). Type B spermatogonia were also characterized by two or more small nucleoli (1.5–2 μm). The nucleolus size of cysts with more than 16 germ cells was smaller than that of cysts with fewer cells (1–1.5 μm). Primary spermatocytes can be identified by multiple nucleoli (≤ 1.5 μm) in the smaller nucleus, and especially at the beginning of meiosis (meiotic prophase I) they are distinct from medaka SYCP1-antibody labeling

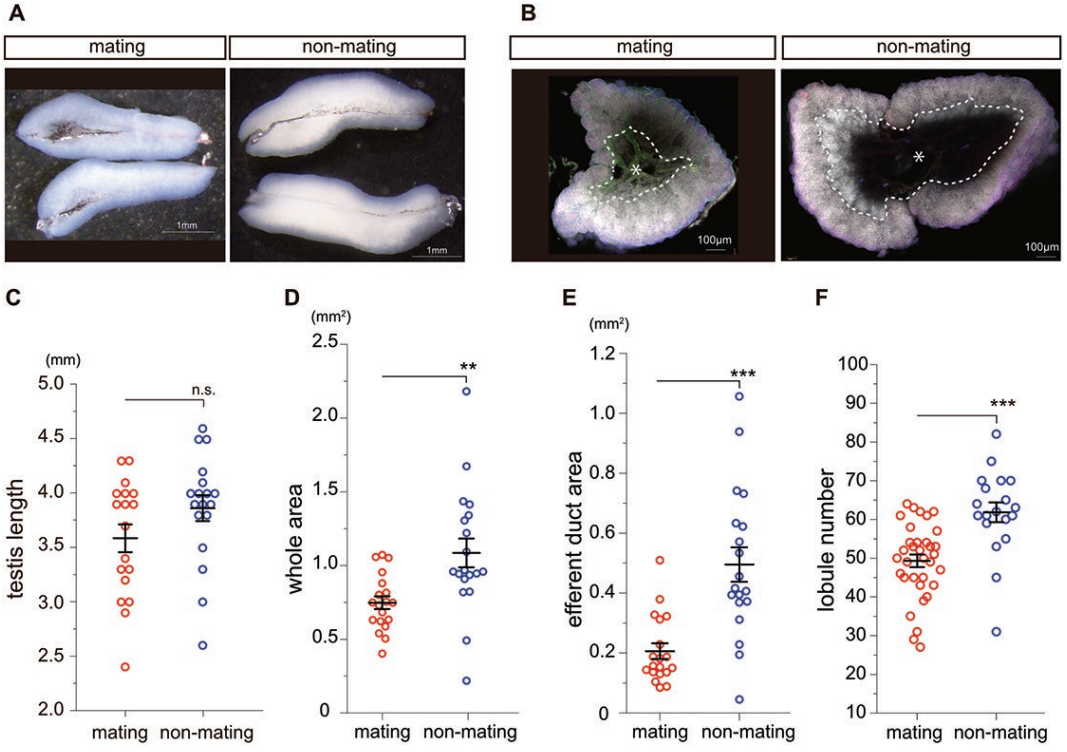

Fig. 2. Differences in testicular morphology under the 'mating' or 'non-mating' conditions. **(A)** Whole appearance of the testis. **(B)** Most central cross-section in the testis (white, DAPI; red, BrdU; green, SYCP1/Laminin; blue, OLVAS; *white dotted line, a boundary between an efferent duct area and a lobule area). **(C)** The length of the anterior-posterior axis. **(D)** The whole testicular area of the most central cross-section. **(E)** The efferent duct area of the most central cross-section. **(F)** The lobule number of the most central cross-section (n = 19 under each condition; bar, average; error bar, S.E.; n.s., $P > 0.05$; **, $P < 0.01$; ***, $P < 0.001$ using Student's t test).

(Iwai et al., 2006; Nakamura et al., 2010). A cyst composed of primary spermatocytes surrounded by Sertoli cells was abbreviated as pSCcys for convenience herein (Fig. 1A). Secondary spermatocytes could be discriminated from primary spermatocytes based on their smaller nucleus and brighter DAPI staining. The nucleolus was hardly recognizable.

Round spermatids possess a nucleus that is 3 μm in size. Further, these spermatids displayed a markedly brighter DAPI staining with chromosome condensation (Saksouk et al., 2015). The nucleolus was no longer visible by DAPI staining.

Whole appearance and histology of 'non-mating' and 'mating' testes

'Non-mating' testis seemed to be more swollen in its outer appearance, with a wider proximal-distal axis than 'mating' testis (Fig. 2A). The whole area of the cross-section at the middle of the testis was larger under the 'non-mating' conditions than 'mating' conditions (Fig. 2B). The length of the anterior-posterior axis tended to be longer in the 'non-mating' testis; however, the difference was not statistically significant (Fig. 2C). However, the whole area of the testis in the cross-sections was significantly larger in the 'non-mating' testis than the 'mating' testis (Fig. 2D). The larger size was due to the expansion of the efferent duct area (Fig. 2E), which was filled with sperm (see Supplementary Figure S3A). The entire area of lobules did not differ between 'non-mating' and 'mating' testes (see Supplementary Figure S3B). Interestingly, the number of lobules per single cross-section was greater in 'non-mating' testis than 'mating' testis (Fig. 2F), implying that the size of single lobules is smaller in 'non-mating' testis than 'mating' testis.

Testicular morphology does not differ along the anterior-posterior axis

We suspected that the sectional morphology of the testis described above might vary along the anterior-posterior axis. To explore this, whole testes were cut into seven ('mating') and four ('non-mating') fragments (see Supplementary Figure S4A), and immunostained using antibodies to OLVAS (germ cell marker), Laminin (outline of lobule), and BrdU (mitotic cells) followed by staining of the nucleic acid with DAPI (see Supplementary Figure S4B, C). Although the number of lobules at the most posterior tip of the testis was small in the 'mating' testis, the sections from other anterior-posterior locations did not significantly differ between 'mating' and 'non-mating' testis (see Supplementary Figure S5A, B). The total number of type A spermatogonia and SGcys per cross-section did not change among the different positions (see Supplementary Figure S5C–F). Therefore, we used all sections cumulatively in later experiments.

The number of mitotic type A spermatogonia, SGcys, and pSCcys decreases in 'non-mating' testis, which likely results in small size of lobule

To explore the cause of the smaller size of lobules in 'non-mating' testis, type A spermatogonia, SGcys, and pSCcys were enumerated. The numbers were found to be lower in 'non-mating' testis compared to 'mating' testis (Fig. 3A–C). Such findings partly explained the smaller area of lobules in 'non-mating' testis.

The histological examination suggested reduced mitotic activity of type A spermatogonia in 'non-mating' testis. To explore this further, a BrdU labeling experiment was performed to confirm the differences in the mitotic activity of type A spermatogonia. Approximately 13% of type A spermatogonia incorporated BrdU by 3 hpB in 'non-mating' testis. However, in 'mating' testis, BrdU-positive type A spermatogonia constituted 22% of the total number of type A spermatogonia (Fig. 4A). Fewer SGcys incorporated BrdU in 'non-mating' than in 'mating' testis (Fig. 4B). The incorporation rates of BrdU by type A spermatogonia and SGcys did not significantly differ at the different anterior-posterior positions (see Supplementary Figure S6A–D), suggesting the uniform distribution of a mitotically active type of type A spermatogonia along the anterior-posterior axis of the testis.

Dynamics of the mitotic activity of germ cells in 'mating' and 'non-mating' testis

Mitotic activity of oogonia including germline stem cells in medaka is divided into two types, active and quiescent oogonia (Nakamura et al., 2010). Therefore, the dynamics of mitotic activity were examined at 1 and 3 hpB, 1, 3, and 8

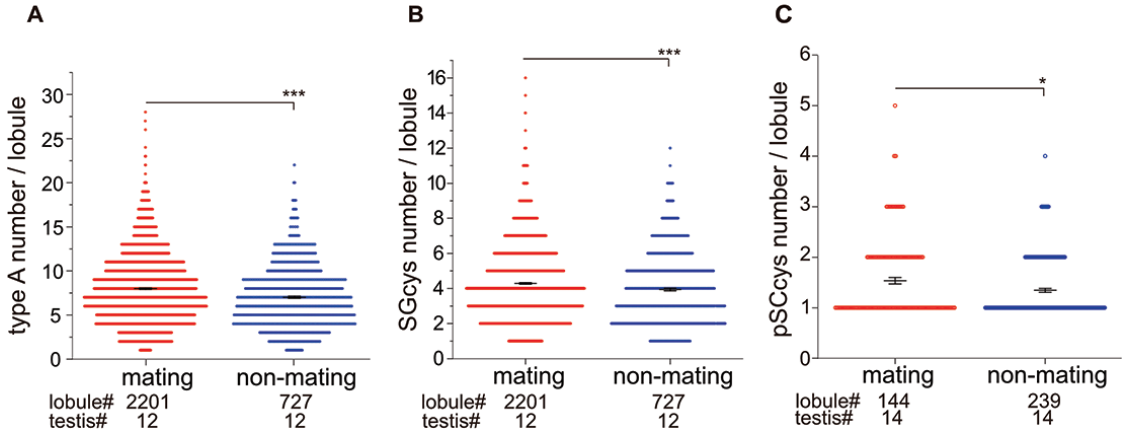

Fig. 3. The decrease of a germ cell number in the 'non-mating' conditions. The numbers of type A spermatogonia **(A)**, SGcys **(B)**, and pSCcys **(C)** per single lobule (bar, average; error bar, S.E.; *, $P < 0.05$; ***, $P < 0.001$ using Student's *t* test).

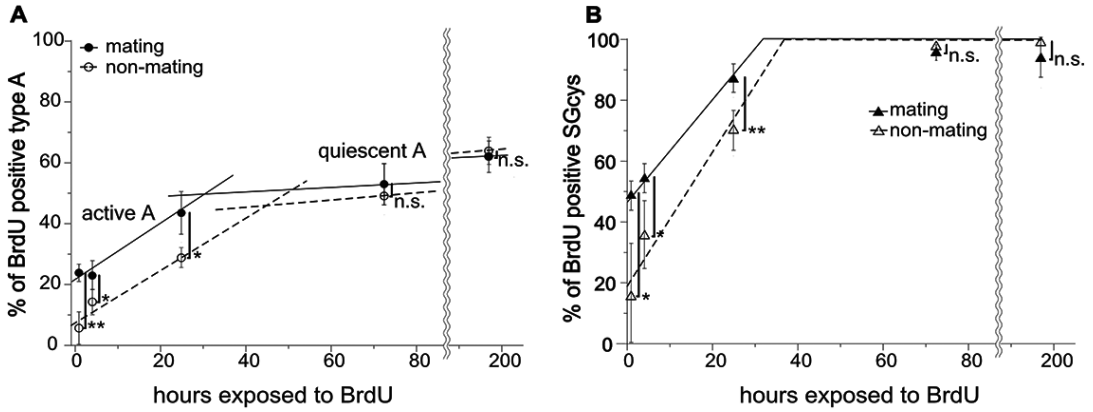

Fig. 4. Piecewise linear regression of the BrdU incorporation rate. BrdU incorporation rate in the nuclei of type A spermatogonia **(A)** and SGcys **(B)** at different time points of BrdU treatment: 1 h (1 hpB), 3 h (3 hpB), 1 day (1 dpB), 3 days (3 dpB), and 8 days (8 dpB). Approximately 30 h was taken by the germ cells in SGcys to be labeled with BrdU (n = 4 at each time point; bar, average; error bar, S.D.; n.s., $P > 0.05$; *, $P < 0.05$; **, $P < 0.01$ using Student's t test).

dpB in testes (long-term labeling experiment). Intriguingly, even after 8 days of treatment, approximately 40% of type A spermatogonia remained unlabeled with BrdU (Fig. 4A). Linear piecewise regression findings also supported the presence of two populations (quiescent and active) of type A spermatogonia in terms of mitotic activity. Given that active type A spermatogonia continuously divide, the cell cycle time for type A spermatogonia was approximately 30 h (Fig. 4A).

In contrast, there were no mitotically inactive germ cells in SGcys. Briefly, they were all labeled with BrdU for approximately 30 h (Fig. 4B). This suggests that once type A spermatogonia are committed to spermatogenesis, they continuously proliferate, with no mitotically resting germ cells in SGcys.

We also analyzed the correlation of the mitotic rate of type A spermatogonia with that of type B spermatogonia in SGcys within single lobules. There was no correlation of BrdU incorporation between type A and type B spermatogonia within a single lobule. The regulation of mitotic activity in single lobules seemed to be independent between type A spermatogonia and SGcys in both 'mating' (see Supplementary Figure S7A) and 'non-mating' (see Supplementary Figure S7B) testis.

The total numbers of A type spermatogonia and SGcys per single cross-section do not change between 'non-mating' and 'mating' conditions

Although the type A spermatogonia and SGcys in a single lobule decreased in 'non-mating' testis, the lobule number in a single cross-section increased (Figs. 2F, 3A and B). This prompted us to examine how many type A spermatogonia and SGcys are present per single cross-section. The total numbers in a single cross-section were calculated by multiplying the lobule number by the average numbers of type A spermatogonia per lobule or SGcys per lobule. Interestingly, the total numbers of type A spermatogonia and SGcys in a single cross-section did not differ between 'non-mating' and 'mating' testes (Fig. 5A, B). These findings suggest that the total numbers of type A spermatogonia and SGcys are maintained regardless of the 'mating' conditions.

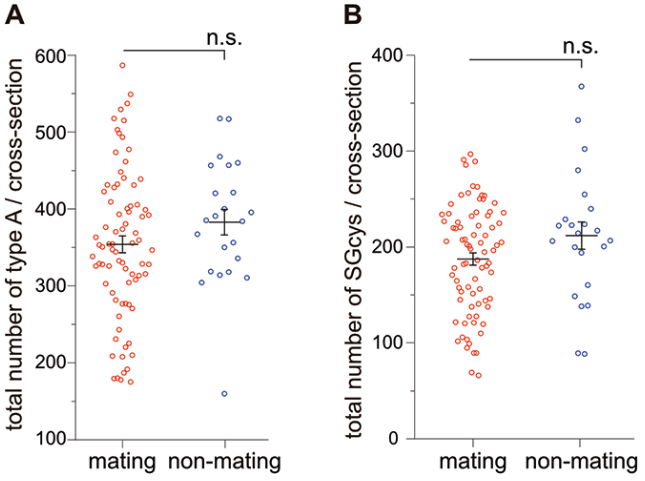

Fig. 5. Total number of spermatogonia per cross-section. Total numbers of type A spermatogonia **(A)** and SGcys **(B)** per single cross-section do not change significantly regardless of the mating conditions (bar, average; error bar, S.E.; n.s., $P > 0.05$ using Student's t test).

Estimated time from type A spermatogonia to sperm

SYCP1 is a component of the synaptonemal complex acting in the prophase of meiotic germ cells (Iwai et al., 2006). Therefore, SYCP1 marks a very early stage in primary spermatocytes. Immunohistochemistry of germ cells with the SYCP1 antibody revealed that the minimal number of SYCP1-positive germ cells in a single pSCcys was 128 (see Supplementary Figure S8). This finding indicates that once spermatogonia are committed to spermatogenesis as type B, type B spermatogonia mitotically divide at least seven times before entering meiosis. As the cell cycle is estimated to be approximately 30 h (Fig. 4A), it takes at least 9 days until type A spermatogonia enter meiosis.

To calculate the time from primary spermatocytes to sperm, a BrdU-chase experiment was performed. BrdU-positive secondary spermatocytes were observed by 2 days after the onset of BrdU treatment in both 'mating' and 'non-mating' conditions (Fig. 6A, B). BrdU-positive round sperma-

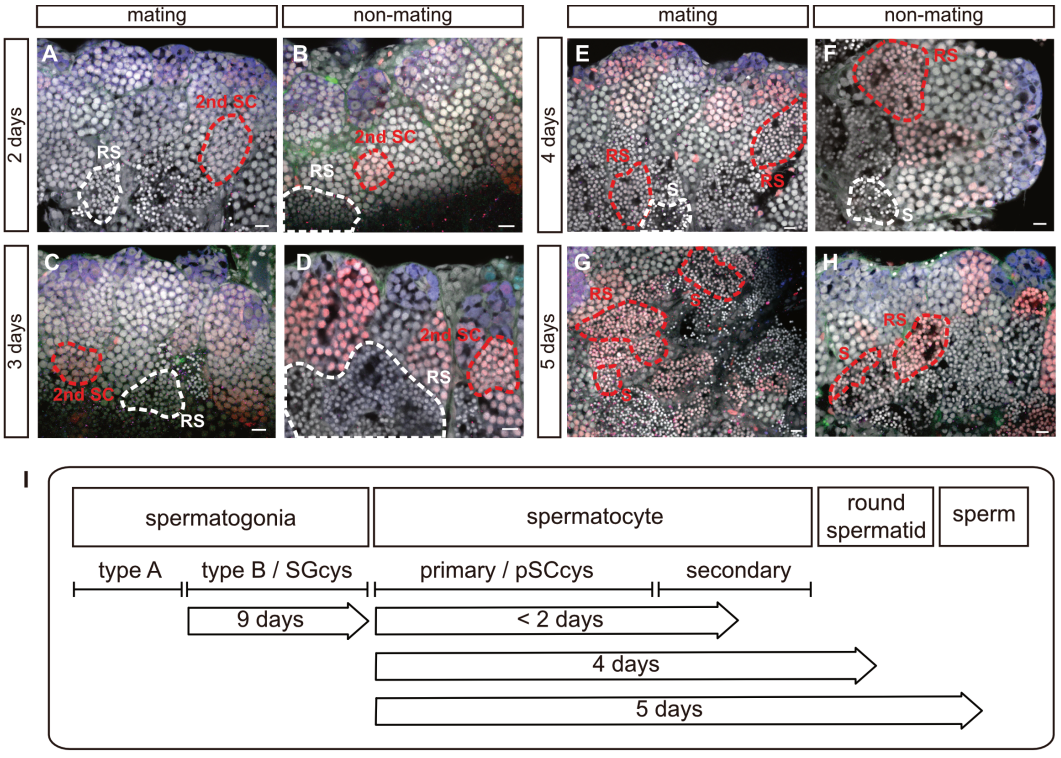

Fig. 6. Estimated time from commitment to spermatogenesis to sperm. **(A, B)** Two days from the onset of BrdU incorporation. **(C, D)** Three days from the onset of BrdU incorporation. **(E, F)** Four days from the onset of BrdU incorporation. **(G, H)** Five days from the onset of BrdU incorporation. (n = 3 **(A–F)**; n = 5 **(G, H)**; 2nd SC, secondary spermatocyte; RS, round spermatid; S, sperm; red dotted lines, BrdU-positive germ cells; white dotted lines, BrdU-negative germ cells; bar, 10 μm; white, DAPI; red, BrdU; green, SYCP1/Laminin; blue, OLVAS). **(I)** Minimum time for spermatogenesis.

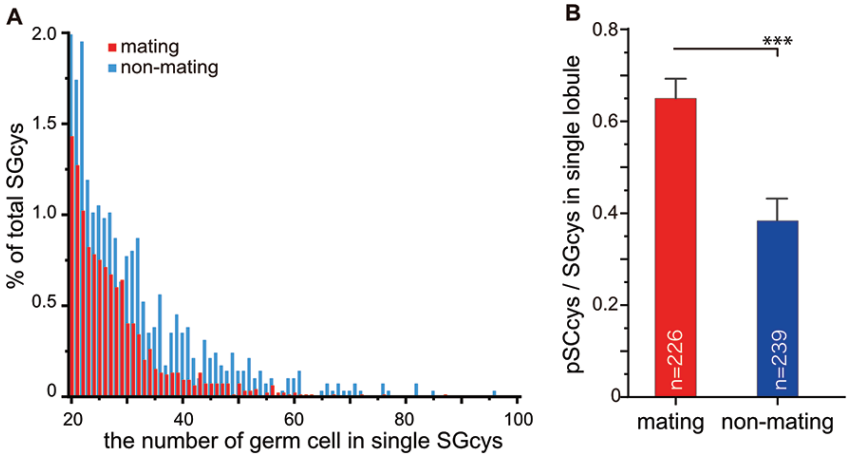

Fig. 7. Increase of SGcys with a large number of type B spermatogonia in the 'non-mating' conditions. **(A)** SGcys distribution and **(B)** ratio of pSCcys to the number of SGcys in a single lobule (bar, average; error bar, S.E.; ***, P < 0.001 using Student's t test).

tids appeared 4 days after the onset of BrdU treatment (Fig. 6E, F). Finally, it took at least 5 days to observe sperm with a BrdU signal (Fig. 6G, H).

Collectively, these data reveal that the time taken by germ cells to proceed from type A spermatogonia to sperm is approximately 14 days, with no significant time difference to reach sperm after entering meiosis between 'mating' and 'non-mating' testes (Fig. 6I).

Commitment to meiosis

During analysis, we noticed a larger ratio of SGcys that had experienced more than four rounds of mitotic division in 'non-mating' testis than 'mating' testis (Fig. 7A). In addition, the ratio of the number of pSCcys to that of SGcys was also significantly smaller in 'non-mating' testis (Fig. 7B). This can be explained by the retarded transition from mitosis to meiosis in 'non-mating' testis.

DISCUSSION

We found that the gross morphology of testis differs between 'non-mating' and 'mating' medaka. However, the 'non-mating' conditions employed were artificial. Therefore, whether these 'non-mating' conditions are relevant to wild habitats is a pertinent question. One possible explanation is that medaka may be isolated after flooding or drought. However, a more likely explanation is that the 'non-mating' status reflects a socially inferior position in medaka schools (Okuyama et al., 2017).

Irrespective of the actual nature of the 'non-mating' conditions, the aim of this study was to reveal the presence of a mechanism that modifies the proliferation of spermatogonia and transition to meiosis, depending on the presence or absence of a mating partner. It is noteworthy that in

Drosophila, the mitotic activity of germline stem cells changes under different mating conditions (Malpe et al., 2020), implying that the partner-dependent homeostasis of spermatogenesis is not unique to medaka.

As the first step to address the cause of this difference, we examined the histology and the dynamics of spermatogenesis. The efferent duct of the 'non-mating' testis was larger than that of the 'mating' testis. The histological examination indicates that spermatogenesis proceeds even in the non-mating state, which may be the reason for testis expansion. Type A spermatogonia took at least 9 days to reach meiotic prophase I and another 5 days to develop sperm. Notably, these times are 6–10 days shorter than those previously reported (Iwasaki et al., 2009). The difference might be due to the performance of in vitro culture experiments in the previous study. In the present study, there was no significant difference in the time for spermatogenesis between the 'non-mating' and 'mating' conditions.

Of note, type A spermatogonia have two mitotic types, a quiescent type and an active type, as previously described in medaka oogenesis (Nakamura et al., 2010). Medaka testis must produce a remarkable number of sperm throughout the reproductive period. It is reasonable to assume that the population of type A spermatogonia contains germline stem cells, although this has not been experimentally proven. Interestingly, we observed different intensities of DAPI staining in the population of type A spermatogonia (Fig. 1B). Such a difference is also described in germline stem cells in mouse testis (Fayomi and Orwig, 2018). In addition, type A spermatogonia were divided into two types according to mitotic activity (Fig. 4A). However, the difference in DAPI staining was not correlated with the difference in mitotic activity (see Supplementary Figure S2B, Fig. 4A), indicating that four different types can be recognized in the population of type A spermatogonia. Unlike in medaka ovaries (Nakamura et al., 2010) and mammalian testes (Kubota and Brinster, 2018), how the different types in medaka testes correspond to any different activity of germline stem cells is unknown.

Correlation analysis data of mitosis between type A spermatogonia and germ cells in SGcys suggest an independent regulation within a single lobule. Since type A spermatogonia are the germ cells critical to give rise to all germ cells, mitosis of type A spermatogonia may be involved in the homeostasis of sperm production. The decreased number of SGcys in 'non-mating' testis may be due to a low number of type A spermatogonia resulting from the reduced mitosis activity of type A spermatogonia. Herein, we did not determine why SGcys with a larger number of spermatogonia accumulated more in 'non-mating' testis (Fig. 7). However, it is possible that meiosis entry is retarded in the 'non-mating' conditions. So far as observed, no increase in apoptosis in the SGcys of 'non-mating' testes was evident. In *Caenorhabditis elegans*, a protein called major sperm protein (MSP), which is expressed in sperm, regulates meiosis in oocytes (Kosinski et al., 2005). It could be possible that the accumulation of sperm in the efferent duct under the 'non-mating' conditions in medaka (Fig. 2E, see Supplementary Figure S3A) regulates the entry into meiosis.

Our collective results suggest that the mitotic regulation of type A spermatogonia and the entry into meiosis may be affected in the absence of a mating partner, which likely contributes to the smaller size of lobules in 'non-mating' testis.

ACKNOWLEDGMENTS

The studies using medaka were supported by a Grant-in-Aid for Scientific Research on Innovative Area (17H06430) and for Scientific Research A (16H02514). We express our gratitude to our lab members for their continued support, especially Drs. Y. Sakae and M. Kikuchi for their valuable discussions.

COMPETING INTERESTS

The authors declare no conflicts of interest.

AUTHOR CONTRIBUTIONS

R.S., T.N. and M.T. designed this study and discussed the results. R.S. performed all the experiments. R.S. and M.T. wrote the manuscript and prepared all tables and figures.

SUPPLEMENTARY MATERIALS

Supplementary materials for this article are available online. (URL: https://doi.org/10.2108/zs210025)

Supplementary Figure S1. Schematic representation of the 'non-mating' and 'mating' conditions.

Supplementary Figure S2. Two types of type A spermatogonia in terms of DAPI intensity: dark A and bright A spermatogonia.

Supplementary Figure S3. Sperm observed in an efferent duct and lobule area.

Supplementary Figure S4. Cross-sections along the anterior-posterior axis.

Supplementary Figure S5. The number of lobules or the number of type A spermatogonia and SGcys per cross-section or a single lobule at different positions.

Supplementary Figure S6. Rate of BrdU incorporation at different positions of a single cross-section along the anterior and posterior axis.

Supplementary Figure S7. Lack of correlation of BrdU uptake between type A spermatogonia and SGcys in single lobules.

Supplementary Figure S8. Example of germ cell enumeration in a single cyst.

REFERENCES

Aoki Y, Nagao I, Saito D, Ebe Y, Kinjo M, Tanaka M (2008) Temporal and spatial localization of three germline-specific proteins in medaka. Dev Dyn 237: 800–807

Iwai T, Yoshii A, Yokota T, Sakai C, Hori H, Kanamori A, et al. (2006) Structural components of the synaptonemal complex, SYCP1 and SYCP3, in the medaka fish *Oryzias latipes*. Exp Cell Res 312: 2528–2537

Iwasaki Y, Ohkawa K, Sadakata H, Kashiwadate A, Takayama WE, Onitake K, et al. (2009) Two states of active spermatogenesis switch between reproductive and non-reproductive seasons in the testes of the medaka, *Oryzias latipes*. Develop Growth Differ 51: 521–532

Fayomi AP, Orwig KE (2018) Spermatogonial stem cells and spermatogenesis in mice, monkeys and men. Stem Cell Res 29: 207–214

Grier HJ (1976) Sperm development in the teleost *Oryzias latipes*. Cell Tissue Res 168: 419–431

Kikuchi M, Nishimura T, Ishishita S, Matsuda Y, Tanaka M (2020) *foxl3*, a sexual switch in germ cells, initiates two independent molecular pathways for commitment to oogenesis in medaka. Proc Natl Acad Sci USA 117: 12174–12181

Kinoshita M, Murata K, Naruse K, Tanaka M (Eds) (2009) A Laboratory Manual for Medaka Biology. Wiley-Blackwell, Hoboken, USA, pp 157–159

Kosinski M, McDonald K, Schwartz J, Yamamoto I, Greenstein D

(2005) *C. elegans* sperm bud vesicles to deliver a meiotic maturation signal to distant oocytes. Development 132: 3357–3369
Kubota H, Brinster RL (2018) Spermatogonial stem cells. Biol Reprod 99: 52–74
Malpe MS, McSwain LF, Kudyba K, Ng CL, Nicholson J, Brady M, et al. (2020) G-protein signaling is required for increasing germline stem cell division frequency in response to mating in *Drosophila* males. Sci Rep 10: 3888
Munakata A, Kobayashi M (2010) Endocrine control of sexual behavior in teleost fish. Gen Comp Endocrinol 165: 456–468
Nakamura S, Kobayashi D, Aoki Y, Yokoi H, Ebe Y, Wittbrodt J, et al. (2006) Identification and lineage tracing of two populations of somatic gonadal precursors in medaka embryos. Dev Biol 295: 678–688
Nakamura S, Kobayashi K, Nishimura T, Higashijima S, Tanaka M (2010) Identification of germline stem cells in the ovary of the teleost medaka. Science 328: 1561–1563
Nakamura S, Watakabe I, Nishimura T, Picard JY, Toyoda A, Taniguchi Y, et al. (2012) Hyperproliferation of mitotically active germ cells due to defective anti-Müllerian hormone signaling mediates sex reversal in medaka. Development 139: 2283–2287
Nishimura T, Nakamura S, Tanaka M (2016) A structurally and functionally common unit in testes and ovaries of medaka (*Oryzias latipes*), a teleost fish. Sex Dev 10: 159–165
Nishimura T, Yamada K, Fujimori C, Kikuchi M, Kawasaki T, Siegfried KR, et al. (2018) Germ cells in the teleost fish medaka have an inherent feminizing effect. PLoS Genet 14: e1007259
Okuyama T, Yokoi S, Takeuchi H (2017) Molecular basis of social competence in medaka fish. Dev Growth Differ 59: 211–218
Onitake K (1972) Morphological studies of normal sex-differentiation and induced sex-reversal process of gonads in the medaka, *Oryzias latipes*. Annot Zool Japon 45: 159–169
Saito D, Morinaga C, Aoki Y, Nakamura S, Mitani H, Furutani-Seiki M, et al. (2007) Proliferation of germ cells during gonadal sex differentiation in medaka: Insights from germ cell-depleted mutant zenzai. Dev Biol 310: 280–290
Sakae Y, Tanaka M (2021) Metabolism and sex differentiation in animals from a starvation perspective. Sex Dev (in press)
Sakae Y, Oikawa A, Sugiura Y, Mita M, Nakamura S, Nishimura T, et al. (2020) Starvation causes female-to-male sex reversal through lipid metabolism in the teleost fish, medaka (*Oryzias latipes*). Biol Open 9: bio050054
Saksouk N, Simboeck E, Déjardin J (2015) Constitutive heterochromatin formation and transcription in mammals. Epigenetics Chromatin 8: 3
Satoh N (1974) An ultrastructural study of sex differentiation in the teleost fish *Oryzias latipes*. J Embryol Exp Morphol 32: 195–215
Schulz RW, de França LR, Lareyre JJ, Le Gac F, Chiarini-Garcia H, Nobrega RH, et al. (2010) Spermatogenesis in fish. Gen Comp Endocrinol 165: 390–411
Shimizu Y, Mita K, Tamura M, Onitake K, Yamashita M (2000) Requirement of protamine for maintaining nuclear condensation of medaka (*Oryzias latipes*) spermatozoa shed into water but not for promoting nuclear condensation during spermatogenesis. Int J Dev Biol 44: 195–199
Tobari Y, Tsutsui K (2019) Effects of social information on the release and expression of gonadotropin-inhibitory hormone in birds. Front Endocrinol 10: 243
Watanabe A, Kobayashi E, Ogawa T, Onitake K (1998) Fibroblast growth factor may regulate the initiation of oocyte growth in the developing ovary of the medaka, *Oryzias latipes*. Zool Sci 15: 531–536

(Received March 23, 2021 / Accepted May 24, 2021 /
Published online July 13, 2021)